Research Article

A novel anticancer property of *Lycium barbarum* polysaccharide in triggering ferroptosis of breast cancer cells

Xing DU[1*], Jingjing ZHANG[1,2*], Ling LIU[1], Bo XU[1], Hang HAN[1], Wenjie DAI[1], Xiuying PEI[1], Xufeng FU[1✉], Shaozhang HOU[2✉]

[1]*Key Laboratory of Fertility Preservation and Maintenance of Ministry of Education, School of Basic Medical Sciences, Ningxia Medical University, Yinchuan 750004, China*

[2]*Department of Clinical Pathology, School of Basic Medical Sciences, Ningxia Medical University, Yinchuan 750004, China*

Abstract: Breast cancer is one of the most malignant tumors and is associated with high mortality rates among women. *Lycium barbarum* polysaccharide (LBP) is an extract from the fruits of the traditional Chinese herb, *L. barbarum*. LBP is a promising anticancer drug, due to its high activity and low toxicity. Although it has anticancer properties, its mechanisms of action have not been fully established. Ferroptosis, which is a novel anticancer strategy, is a cell death mechanism that relies on iron-dependent lipid reactive oxygen species (ROS) accumulation. In this study, human breast cancer cells (Michigan Cancer Foundation-7 (MCF-7) and MD Anderson-Metastatic Breast-231 (MDA-MB-231)) were treated with LBP. LBP inhibited their viability and proliferation in association with high levels of ferroptosis. Therefore, we aimed to ascertain whether LBP reduced cell viability through ferroptosis. We found that the structure and function of mitochondria, lipid peroxidation, and expression of solute carrier family 7 member 11 (SLC7A11, also known as xCT, the light-chain subunit of cystine/glutamate antiporter system X_c^-) and glutathione peroxidase 4 (GPX4) were altered by LBP. Moreover, the ferroptosis inhibitor, Ferrostatin-1 (Fer-1), rescued LBP-induced ferroptosis-associated events including reduced cell viability and glutathione (GSH) production, accumulation of intracellular free divalent iron ions and malondialdehyde (MDA), and down-regulation of the expression of xCT and GPX4. Erastin (xCT inhibitor) and RSL3 (GPX4 inhibitor) inhibited the expression of xCT and GPX4, respectively, which was lower after the co-treatment of LBP with Erastin and RSL3. These results suggest that LBP effectively prevents breast cancer cell proliferation and promotes ferroptosis via the xCT/GPX4 pathway. Therefore, LBP exhibits novel anticancer properties by triggering ferroptosis, and may be a potential therapeutic option for breast cancer.

Key words: *Lycium barbarum* polysaccharide; Ferroptosis; Breast cancer cells; xCT; Glutathione peroxidase 4 (GPX4)

1 Introduction

Breast cancer is one of the most malignant tumors in women worldwide. Breast cancer patients present with a high mortality rate owing to the high metastasis and invasion rates of breast cancer cells (Tabor et al., 2020). Breast cancers are categorized into three main groups based on cellular markers: (1) estrogen receptor (ER)- or progesterone receptor (PR)-positive,

(2) human epidermal growth factor receptor 2 (HER2)-positive, and (3) triple-negative breast cancer (TNBC), defined by the absence of ER, PR, and HER2 expression (Kumar and Aggarwal, 2016; Xu et al., 2020). The therapeutic effects of targeted drugs based on these subtypes are significantly stronger than those of conventional treatments of breast cancer involving surgery, chemotherapy, and radiation therapy. However, these targeted anticancer therapies have several limitations such as their adverse side effects, high cost, and drug resistance (Abotaleb et al., 2018). In addition, the development of tumor immunotherapy has improved the prognosis of patients with advanced breast cancer in recent years. However, the safety and efficacy of tumor immunotherapy require validation through clinical trials with large sample sizes (García-Aranda and Redondo, 2019). Although systemic treatments of

✉ Xufeng FU, fuxufeng100@163.com
   Shaozhang HOU, houshzh@nxmu.edu.cn

* The two authors contributed equally to this work

   Xing DU, https://orcid.org/0000-0003-2683-4524
   Xufeng FU, https://orcid.org/0000-0002-4101-1000

breast cancer through chemotherapy, endocrine therapy, targeted therapy, and immunotherapy are effective, there is a need to develop more effective and less toxic novel drugs, and then to optimize existing treatments to improve the prognosis of breast cancer and the quality of life for breast cancer patients (Arzi et al., 2020).

The anticancer effects of several therapies are attributed to cell cycle arrest, an increase in cancer cell death, the inhibition of proliferation, invasion and cell migration, and other signal transductions (Shin et al., 2019; Tavsan and Kayali, 2019). Apoptosis and autophagy are forms of programmed cell death and the preferred targets for anticancer compounds (Greco et al., 2021). Several studies reported additional anticancer strategies through non-canonical cell death such as ferroptosis, which is independent of changes in the apoptosis process (Greco et al., 2021; Bai et al., 2022). Ferroptosis is characterized by the iron-dependent accumulation of lipid reactive oxygen species (ROS) (Dixon et al., 2012). Morphologically, ferroptotic cells are characterized by the shrinkage of mitochondria and depletion of mitochondrial cristae. They do not present typical apoptotic features such as cytoplasmic swelling or disruption of the cell membrane and the formation of autophagic vacuoles (Dixon et al., 2012). In addition, ferroptosis is characterized by accumulation of lipid ROS and free iron ions (Li et al., 2020). Ferroptosis is caused by the inactivation of glutathione peroxidase 4 (GPX4) or inhibition of the light-chain subunit of cystine/glutamate antiporter system X_c^- (xCT). System X_c^- is a cysteine glutamate antiporter which mainly regulates the exchange of intracellular glutamate and extracellular cysteine, thereby modulating the synthesis of glutathione (GSH), which plays an important role in antioxidant activity (Bridges et al., 2012; Yu and Long, 2016). Inhibition of GPX4 causes lipid ROS accumulation and ferroptosis activation (Yang et al., 2014, 2016).

The current breast cancer therapies have several limitations; therefore, there is a need to explore new and effective anticancer strategies and anti-tumor drugs. Currently, several studies are investigating anti-tumor drugs with high efficacy and low toxicity from natural sources. Notably, compounds extracted from plants have been used to develop new anticancer drugs such as paclitaxel, lentinan, and camptothecin (Ijaz et al., 2018). Traditional Chinese herbs have attracted significant attention owing to their anticancer

properties. *Lycium barbarum* polysaccharide (LBP) is extracted from the fruit of the traditional Chinese herb *L. barbarum*. LBP has anti-tumor activity and can enhance the immune response owing to its antioxidant efficacy and activity in stimulating release of endogenous factors (Amagase and Farnsworth, 2011; Deng et al., 2018). LBP inhibits the growth of transplanted sarcoma and hepatoma cells in tumor-bearing mice by enhancing the immunity of the mice. The treatment induces proliferation of lymphocytes, including T lymphocytes, and increases macrophage phagocytosis (Gan et al., 2004; Zhu and Zhang, 2006).

Previous findings reported that LBP inhibits the growth of hepatoma cells (Zhang et al., 2005; Deng et al., 2018), gastric cancer cells (Miao et al., 2010; Chen et al., 2017), bladder cancer cells (Zhang et al., 2017), prostate cancer cells (Luo et al., 2009), cervical cancer cells (Zhu and Zhang, 2013), hemangioma endothelial cells (Lou et al., 2019), colon cancer cells (Mao et al., 2011), skin squamous cell carcinoma cells (Zeng et al., 2019), and breast cancer cells (Shen and Du, 2012; Cumaoglu et al., 2018). Inhibition is achieved by inducing apoptosis, autophagy, and other multiple pathways such as inhibition of cellular proliferation, angiogenesis, and metastasis. In addition, immunomodulatory effects of LBP play important roles in the anti-cancer process (Feng et al., 2020). An anti-tumor effect of some polysaccharides such as fucoidan and β-glucans has been previously reported (Corso et al., 2021; Greco et al., 2021). However, the detailed mechanism of the action of LBP on tumor inhibition, including whether it induces or regulates other forms of programmed death of cancer cells, has not been fully explored.

2 Methods and materials

2.1 Preparation of LBP

LBP was purchased from Shanghai Yuanye Bio-Technology Co., Ltd. (Shanghai, China). A 10.0 mg/mL stock solution of LBP was prepared in Dulbecco's modified Eagle's medium (DMEM; Gibco BRL, Grand Island, NY, USA) and stored at −20 °C. Final concentrations for testing were prepared by dilution of the stock solution using DMEM for all experiments, whereas an equivalent volume of DMEM was used for the control group.

2.2 Cell culture and treatments

Human breast cancer cell lines Michigan Cancer Foundation-7 (MCF-7) and MD Anderson-Metastatic Breast-231 (MDA-MB-231) were purchased from the Shanghai Cell Bank of the Chinese Academy of Sciences. The two cell lines were cultured in DMEM supplemented with 10% (volume fraction) fetal bovine serum (Gibco BRL) and 1% (0.01 g/mL) penicillin/streptomycin (Gibco BRL) in an incubator with 5% CO_2 at 37 ℃. After achieving a cell fusion rate of 80%, samples were digested with 2.5 g/L trypsin (Gibco BRL) and passaged in new dishes. The cells were seeded and cultured for 12 h to adhere to the culture dish. They were then exposed to serial concentrations of LBP for various time points, and cell adherence and survival status were observed under a microscope (Nikon, Japan). Final concentrations of 10 μmol/L Ferrostatin-1 (Fer-1; Selleckchem, USA), 10 μmol/L Erastin (MedChemExpress, Shanghai, China), and 5 μmol/L RSL3 (MedChemExpress) were incubated for 48 h with LBP or independently.

2.3 Determination of cell viability

The viability of the MCF-7 and MDA-MB-231 cells was assayed using a cell counting kit-8 (CCK-8; APExBIO Technology, USA) according to the manufacturer's instructions. In summary, the cells were seeded in 96-well plates at a density of 5000 cells/well for 24 h. DMEM containing serial concentrations of LBP was added for viability determination experiments. After exposure to LBP at indicated time points, the medium was replaced with fresh medium and incubated with 10% (volume fraction) kit reagent at 37 ℃ for 2 h. Absorbance (optical density (OD) value) of each well was measured at 450 nm using a microplate reader (Thermo Scientific, Boston, USA). The average of three independent tests was calculated to determine the effect of LBP on the viability of the breast cancer cells.

2.4 RNA-sequencing

Total RNA was extracted from the control and 8.0 mg/mL LBP-treated groups (*n*=3) using TRIzol reagent (TaKaRa, China) according to the manufacturer's instructions. Sequencing of RNA samples was conducted by Xuanchen Biological Technology Co., Ltd. (Shaanxi, China). RNA purity was determined using a NanoPhotometer spectrophotometer (Implen, CA,

USA) and RNA integrity was assessed with a Bioanalyzer 2100 system (Agilent Technologies, CA, USA). Sequencing libraries were constructed using an RNA Library Prepare Kit for Illumina (New England Biolabs (NEB), USA) according to the manufacturer's instructions. In summary, messenger RNA (mRNA) was purified from the total RNA using poly-T oligo-attached magnetic beads. The first-strand of complementary DNA (cDNA) was synthesized using a random hexamer primer and reverse transcriptase (ribonuclease H (RNase H)), and the second-strand was subsequently synthesized using DNA polymerase I and RNase H. The library quality of PCR products was assessed using an Agilent Bioanalyzer 2100 system. Library fragments were sequenced on an Illumina Novaseq platform according to the manufacturer's instructions.

2.5 Differential gene expression annotation

Raw data from RNA-sequencing were processed using in-house Perl scripts and clean reads were obtained by removing adapter reads and low-quality reads. To explore gene expression levels, all clean reads were annotated by mapping them to the human reference genome. The reads per kilo bases per million reads (RPKM) were used to calculate the number of expression tags, and differentially expressed genes were identified based on an adjusted *P*-value of <0.05. Pathways associated with differentially expressed genes were identified using the Kyoto Encyclopedia of Genes and Genomes (KEGG) analysis.

2.6 Transmission electron microscopy (TEM)

The morphology of mitochondria was assessed using transmission electron microscope (Hitachi, Tokyo, Japan). After treatment of MCF-7 cells with 8.0 mg/mL LBP for 48 h, $1×10^6$ cells were collected and fixed in 2.5% (volume fraction) glutaraldehyde for 24 h at 4 ℃. The cells were treated with 1% (volume fraction) OsO_4 for 1 h and then dehydrated with absolute ethyl alcohol before embedding them in Epon resin. Ultra-thin sections were then visualized under a transmission electron microscope at 80 kV.

2.7 Determination of mitochondrial membrane potential (MMP)

The MMP was determined using a JC-1 fluorescent probe assay kit (Beyotime Biotechnology, Shanghai, China) according to the manufacturer's instructions. In summary, $1×10^5$ MCF-7 and MDA-MB-231 cells

were seeded in 12-well plates and cultured for 24 h. The culture medium was replaced with fresh medium, and JC-1 working solution was added and incubated for 30 min at 37 °C. Cells were washed three times with phosphate-buffered saline (PBS) and visualized under a fluorescence microscope (Nikon, Japan).

2.8 Lipid ROS determination

A C11-BODIPY 581/591 molecular probe was used to determine the lipid peroxidation activity of LBP on MCF-7 and MDA-MB-231 cells. Cells were incubated at a final concentration of 2 µmol/L in serum-free medium for 20 min, washed three times with PBS, and visualized under a fluorescence microscope at 590 and 510 nm for imaging, according to the manufacturer's instructions.

2.9 Intracellular iron analysis

An iron assay kit (Jiancheng Biotech., Nanjing, China) was used for determination of intracellular iron levels. In summary, 1×10^6 cells were collected and washed three times with PBS, and then lysed with protein lysis buffer on ice for 20 min. After centrifugation for 15 min at 12 000 r/min and 4 °C, the supernatant was collected and analyzed based on the 2 mg/L-iron standard solution of the kit. The total protein concentration in samples was quantified using a BCA protein assay kit (Beyotime, Jiangsu, China). The concentration of intracellular iron was calculated and the unit converted into µmol/g protein according to the manufacturer's instructions.

2.10 Western blotting analysis

MCF-7 and MDA-MB-231 cell lines were treated with 2.5 g/L trypsin and washed three times with PBS. Ice-cold radioimmunoprecipitation assay (RIPA) lysis buffer (Beyotime) containing protease inhibitor cocktails (Beyotime) was added to the cells, and the mixture was incubated on ice for 20 min. The mixture was centrifuged at 12 000 r/min for 15 min at 4 °C. The supernatant was obtained and the total protein concentration of the samples was determined using a BCA protein assay kit (Beyotime). Protein samples (30 µg/well) were denatured at 100 °C for 10 min, then separated by 0.125 g/mL sodium dodecyl sulphate-polyacrylamide gel electrophoresis (SDS-PAGE) and electro-transferred onto polyvinylidene difluoride (PVDF) membranes (EMD Millipore, Billerica, MA, USA) at a constant voltage of 100 V for 2 h. The

PVDF membranes of the immunoblots were blocked with 0.05 g/mL non-fat milk dissolved in Tris-buffered solution containing 1% (volume fraction) Tween 20 (TBST) for 2 h. They were then incubated with primary antibodies (diluted to 1:1000 (volume ratio)) at 4 °C overnight and washed three times for 5 min each time with TBST. The membranes were further incubated with horseradish peroxidase (HRP)-conjugated secondary antibody for 1 h and washed three times with PBST (Du et al., 2021). The signal was detected using an electrochemilu-minescence (ECL) chemiluminescence kit (Thermo Scientific) with a fluorescence detection device (Thermo Scientific). Antibodies against cyclin-dependent kinase inhibitor 1A (p21), xCT, and GPX4 were purchased from the Cell Signaling Technology Co. (Abcam, Cambridge, UK), and the reference antibodies (glyceraldehyde-3-phosphate dehydrogenase (GAPDH), tubulin, and β-actin) were purchased from Beyotime. All primary antibodies were diluted to 1:1000 (volume ratio). Representative images were selected from at least three independent experiments.

2.11 Statistical analysis

For quantitative analysis of protein expression, quantification of target proteins and an internal reference protein (β-actin, tubulin, or GAPDH) was performed using ImageJ software (National Institutes of Health, USA). Ratios of the expression levels of the target proteins and internal reference protein are presented as mean±standard deviation (SD) using GraphPad Prism 6 (GraphPad Software, Inc., San Diego, CA, USA). The data (including cell viability and malondialdehyde (MDA), GSH, and Fe^{2+} levels) from samples in each group were subjected to normality tests before analysis of variance (ANOVA) or *t*-test analysis using GraphPad Prism 6 software. Comparative analysis of various factors was performed using two-way ANOVA, and multiple samples were compared by one-way ANOVA, using the least significant difference (LSD) method. A *P*-value of <0.05 was considered statistically significant.

3 Results

3.1 Cytotoxic and inhibitory effects of LBP on proliferation of MCF-7 and MDA-MB-231 cells

To explore the cytotoxic and inhibitory effects of LBP on proliferation of breast cancer cells, MCF-7

and MDA-MB-231 cell lines were treated with serial concentrations of LBP (0, 0.4, 0.8, 1.2, 1.6, 2.0, 4.0, 6.0, 8.0, and 10.0 mg/mL) for different time points. CCK-8 assays were performed to explore cell viability. The findings showed that viability and proliferation of MCF-7 and MDA-MB-231 cells were significantly inhibited by LBP concentrations above 4.0 mg/mL (Figs. 1a and 1b). Treatment for 48 h showed the highest effect and therefore was selected as the treatment time

for subsequent experiments. Morphological analyses of MCF-7 and MDA-MB-231 cells showed that LBP significantly inhibited the viability of the breast cancer cells (Fig. 1c). A colony-formation assay of the cells was performed to explore the anti-proliferative effect of LBP. The findings showed that the colony-formation efficiency of the two cell lines was significantly suppressed by LBP (Figs. 1d and 1e), indicating that LBP inhibited the proliferation of breast cancer cells. To
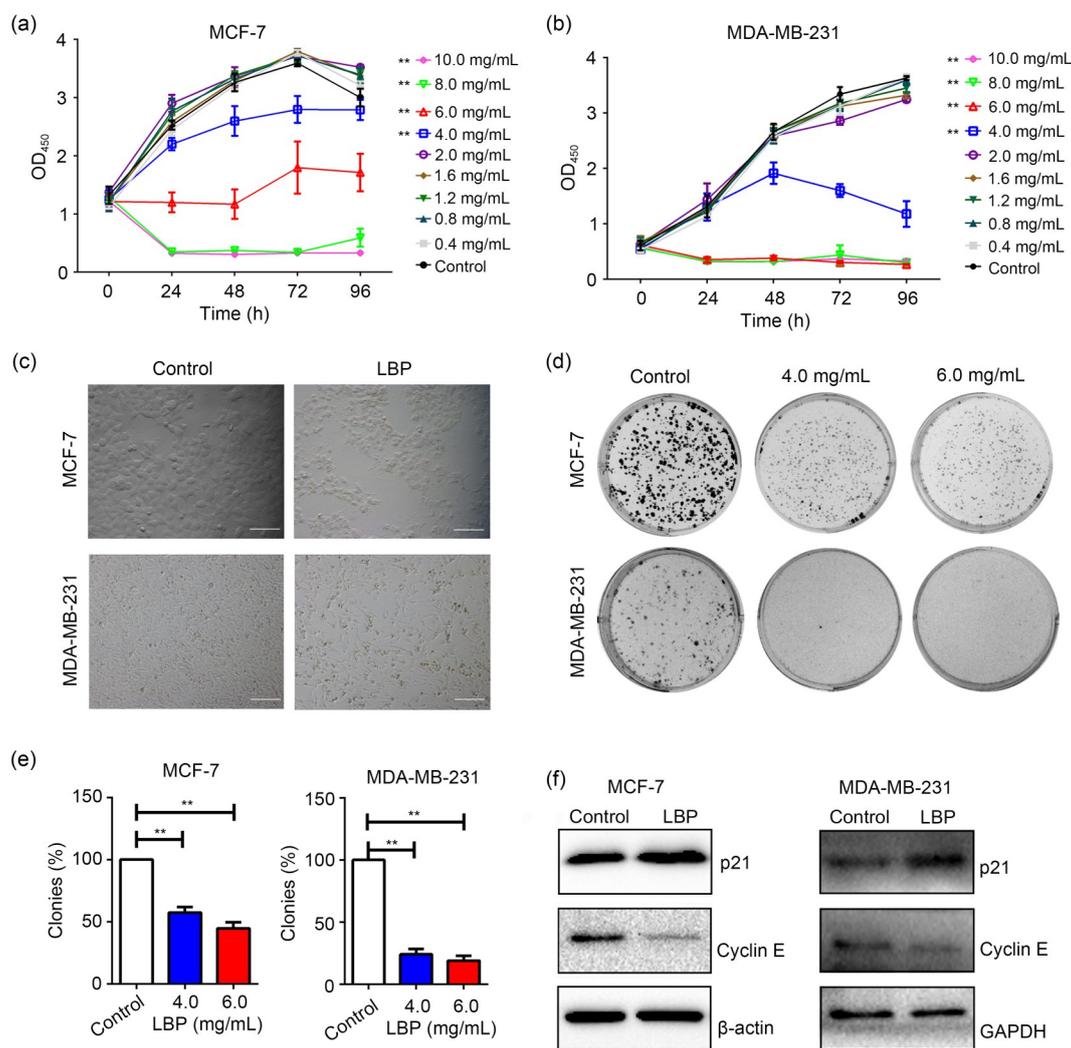

Fig. 1 Inhibitory effects of *Lycium barbarum* polysaccharide (LBP) on the viability and proliferation of MCF-7 and MDA-MB-231 breast cells in vitro. (a) Viability of MCF-7 cells after treatment with LBP; (b) Viability of MDA-MB-231 cells after treatment with LBP; (c) Morphology of MCF-7 and MDA-MB-231 cells after treatment with LBP (scale bar= 200 μm); (d) Colony-formation assays of MCF-7 and MDA-MB-231 cells after treatment with LBP; (e) Quantification of colony-formation assay in (d); (f) Expression levels of cyclin-dependent kinase inhibitor 1A (p21) and Cyclin E in MCF-7 and MDA-MB-231 cells after treatment with 4.0 and 6.0 mg/mL LBP, respectively. Data are expressed as mean±standard deviation (SD), *n*=5. (a, b) ** *P*<0.01 for LBP treatment compared with control, according to the Kruskal-Wallis test of two-way analysis of variance (ANOVA). (e) ** *P*<0.01. OD$_{450}$: optical density at 450 nm; GAPDH: glyceraldehyde-3-phosphate dehydrogenase.

further explore whether LBP inhibited cell proliferation by inducing cell cycle arrest, the expression levels of cell cycle regulatory proteins p21 and Cyclin E were determined. The findings showed that expression of p21 was up-regulated, whereas expression of Cyclin E was down-regulated by LBP in MCF-7 and MDA-MB-231 cells (Fig. 1f). These findings indicated that LBP arrested the cells at the G0/G1-phase of the cell cycle. In summary, LBP could effectively reduce viability and induce cell death and G0/G1-phase arrest in the breast cancer cells.

3.2 Contribution of ferroptosis to LBP-induced cell death in MCF-7 cells

To explore the mechanisms of LBP-induced cell death in breast cancer cells, RNA-sequencing of 8.0 mg/mL LBP-treated MCF-7 cells was performed. The findings showed a total of 1318 differentially expressed genes, of which 632 were down-regulated and 686 up-regulated (Fig. 2a). Differentially expressed genes and their classification are presented in a heatmap (Fig. 2b). Furthermore, KEGG pathway enrichment analyses were performed and the findings showed
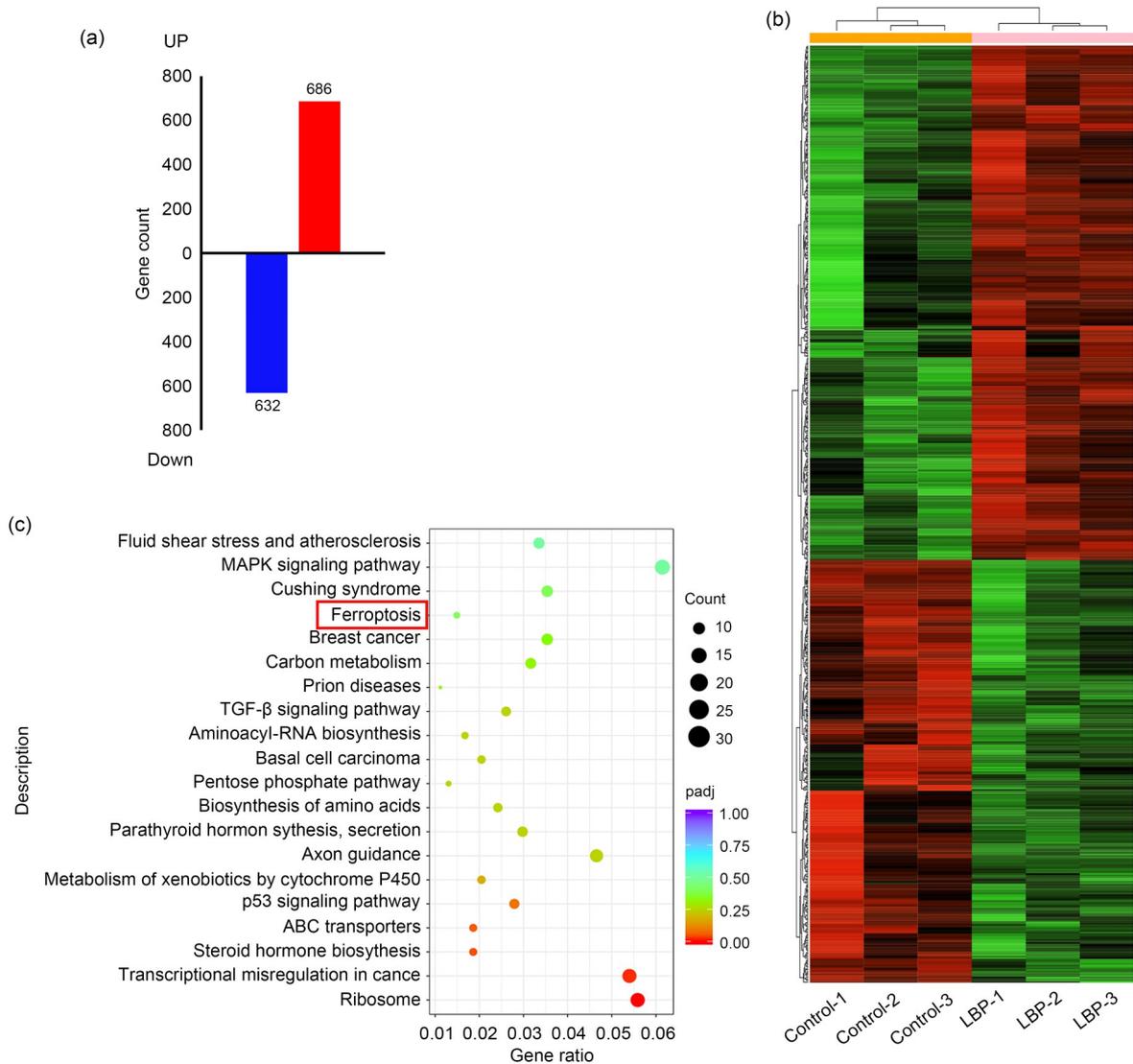

Fig. 2 Enrichment of differentially expressed genes in 8.0 mg/mL *Lycium barbarum* polysaccharide (LBP)-treated MCF-7 cells in the ferroptosis pathway. (a) Differentially expressed genes after LBP treatment compared with control; (b) Heatmap comparing differentially expressed genes in the LBP-treated and control groups (three independent samples in each group); (c) Enriched Kyoto Encyclopedia of Genes and Genomes (KEGG) pathway associated with differentially expressed genes.

that the ferroptosis pathway was significantly enriched (Fig. 2c). These implied that ferroptosis may be a key mediator in LBP-induced breast cancer cell death.

3.3 Effects of LBP on mitochondrial structure and function and the production of lipid ROS in MCF-7 and MDA-MB-231 cells

To verify that LBP killed breast cancer cells through ferroptosis, the characteristics of ferroptosis including mitochondrial structure and function were explored by TEM and a JC-1 fluorescent probe, respectively. Analysis of mitochondrial structure showed shrinkage or matrix condensation, an increase in outer membrane density, and a decrease or disappearance of cristae in MCF-7 cells after treatment with 8.0 mg/mL LBP (Fig. 3a). Analysis of MMP showed a transition from red to green fluorescence after LBP treatment in MCF-7 cells (Fig. 3b) and MDA-MB-231 cells (Fig. 3c), indicating that LBP induced a reduction in MMP in the breast cancer cells.

Lipid peroxidation is a key event in ferroptosis, and therefore was detected using a C11-BODIPY 581/591 molecular probe. The findings showed that the intensity of red fluorescence decreased and the intensity of green fluorescence increased after treatment of MCF-7 cells with 4.0 mg/mL LBP (Fig. 4a) and after treatment of MDA-MB-231 cells with 6.0 mg/mL LBP (Fig. 4b). The findings indicated that LBP induced an increase of the oxidized form and a decrease of the reduced form of iron in the breast cancer cells.

3.4 Effects of ferroptosis inhibitor Fer-1 on LBP-induced ferroptosis in MCF-7 and MDA-MB-231 cells

To further explore the induction of ferroptosis by LBP in breast cancer cells, the cells were co-cultured with the ferroptosis inhibitor Fer-1 and LBP. Ferroptosis events including cell viability, MDA and GSH production, and intracellular free divalent iron accumulation were then detected. The findings showed that Fer-1 rescued cell viability (Figs. 5a and 5b), MDA and GSH levels (Figs. 5c–5f), and intracellular free iron accumulation (Figs. 5g and 5h), which were affected by 4.0 mg/mL LBP in MCF-7 cells and 6.0 mg/mL LBP in MDA-MB-231 cells. The findings indicated that LBP affects the proliferation and viability of breast cancer cells through the ferroptosis pathway.

3.5 LBP-induced ferroptosis by modulating xCT and GPX4 expression

Expression levels of the negative regulatory proteins for ferroptosis, xCT (SLC7A11) and GPX4, were determined by western blotting in MCF-7 and MDA-MB-231 cells to explore the mechanism of LBP-induced ferroptosis of breast cancer cells. The findings showed that LBP significantly down-regulated expression of xCT and GPX4 at various concentrations (2.0, 4.0, 6.0, 8.0, and 10.0 mg/mL) in a dose-dependent manner compared with the control group in MCF-7 cells (Figs. 6a–6c) and MDA-MB-231 cells (Figs. 6d–6f).
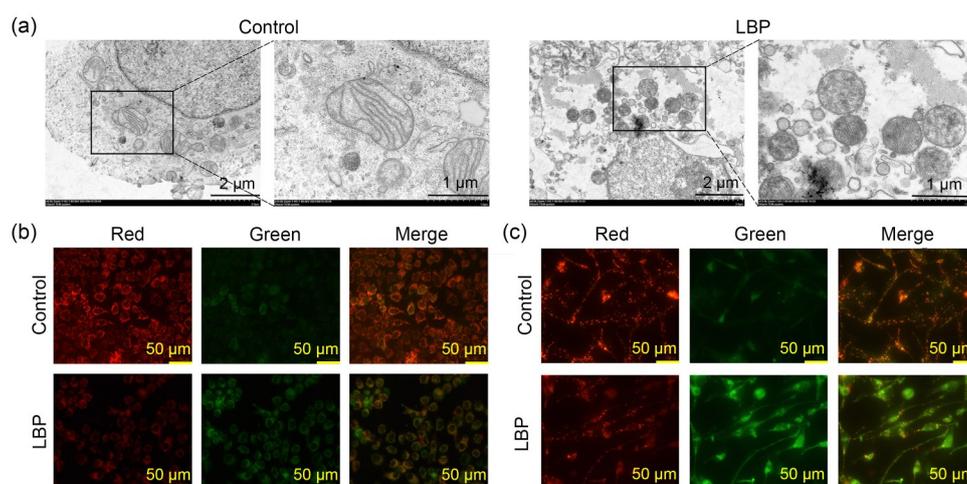

Fig. 3 Effects of *Lycium barbarum* polysaccharide (LBP) on mitochondrial structure and function and the production of lipid reactive oxygen species (ROS) in breast cancer cells. (a) Mitochondrial structure observed under transmission electron microscopy (TEM) in MCF-7; (b) Mitochondrial membrane potential (MMP) determined by JC-1 fluorescent probe in MCF-7 cells; (c) MMP determined by JC-1 fluorescent probe in MDA-MB-231 cells.
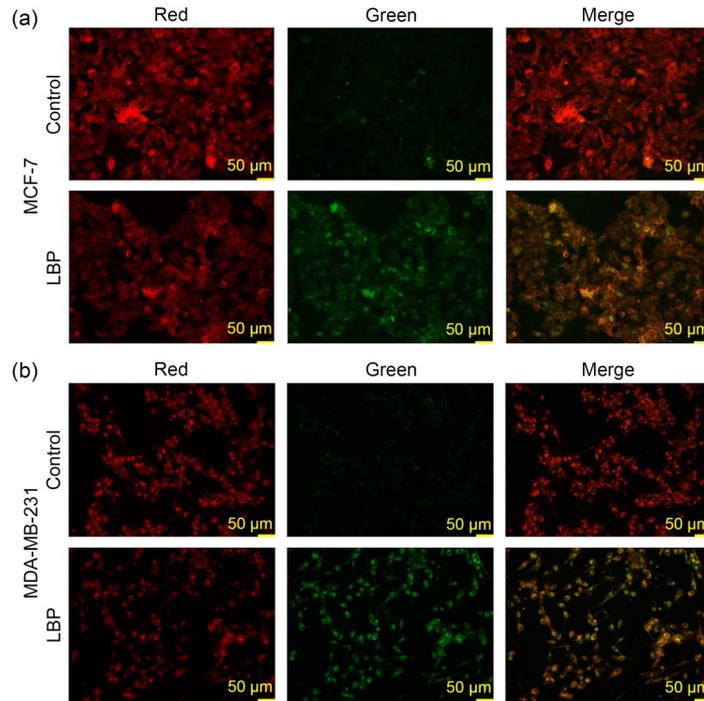
Fig. 4 Lipid peroxidation determined by C11-BODIPY 581/591 molecular probe after 4.0 mg/mL *Lycium barbarum* polysaccharide (LBP) treatment in MCF-7 cells (a) and after 6.0 mg/mL LBP treatment in MDA-MB-231 cells (b).
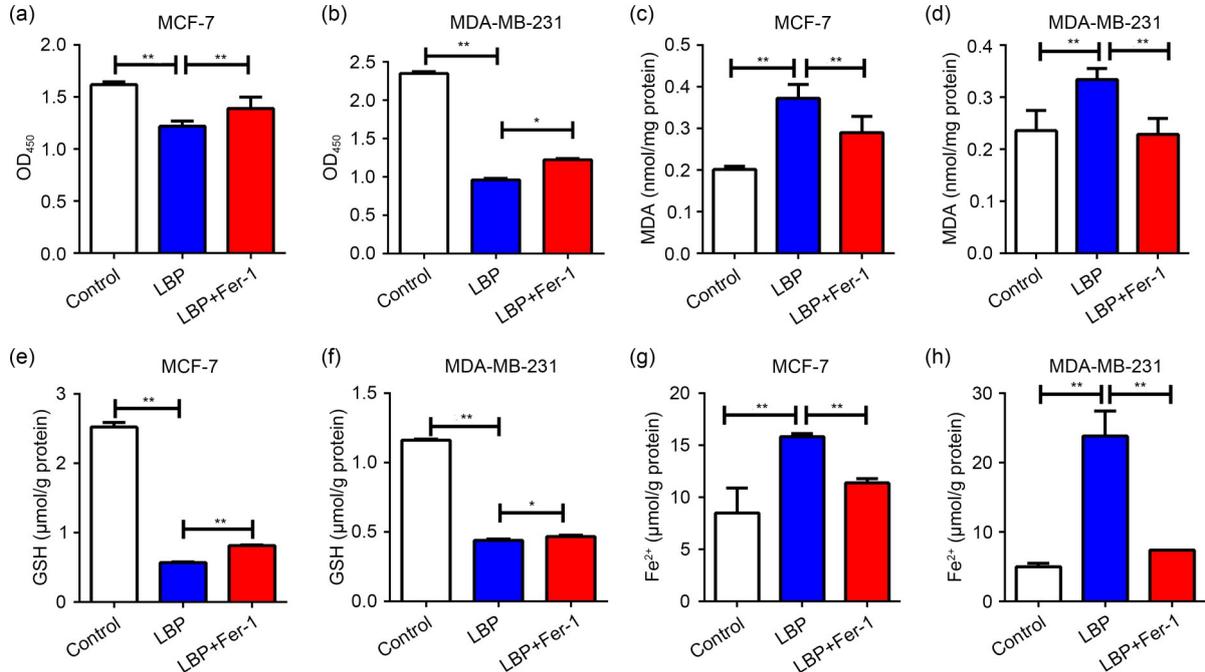

Fig. 5 Effects of ferroptosis inhibitor Ferrostatin-1 (Fer-1) on *Lycium barbarum* polysaccharide (LBP)-induced ferroptosis. (a, b) Fer-1 rescues the decreased cell viability induced by LBP in MCF-7 and MDA-MB-231 cells; (c, d) Fer-1 rescues increased malondialdehyde (MDA) levels induced by LBP in MCF-7 and MDA-MB-231 cells; (e, f) Fer-1 rescues decreased glutathione (GSH) levels induced by LBP in MCF-7 and MDA-MB-231 cells; (g, h) Fer-1 rescues increased intracellular free iron levels induced by LBP in MCF-7 and MDA-MB-231 cells. LBP is 4.0 mg/mL in MCF-7 cells and 6.0 mg/mL in MDA-MB-231 cells; Fer-1 is 10.0 μmol/L in both MCF-7 and MDA-MB-231 cells. Data are expressed as mean±standard deviation (SD), $n=3$. * $P<0.05$, ** $P<0.01$. OD_{450}: optical density at 450 nm.
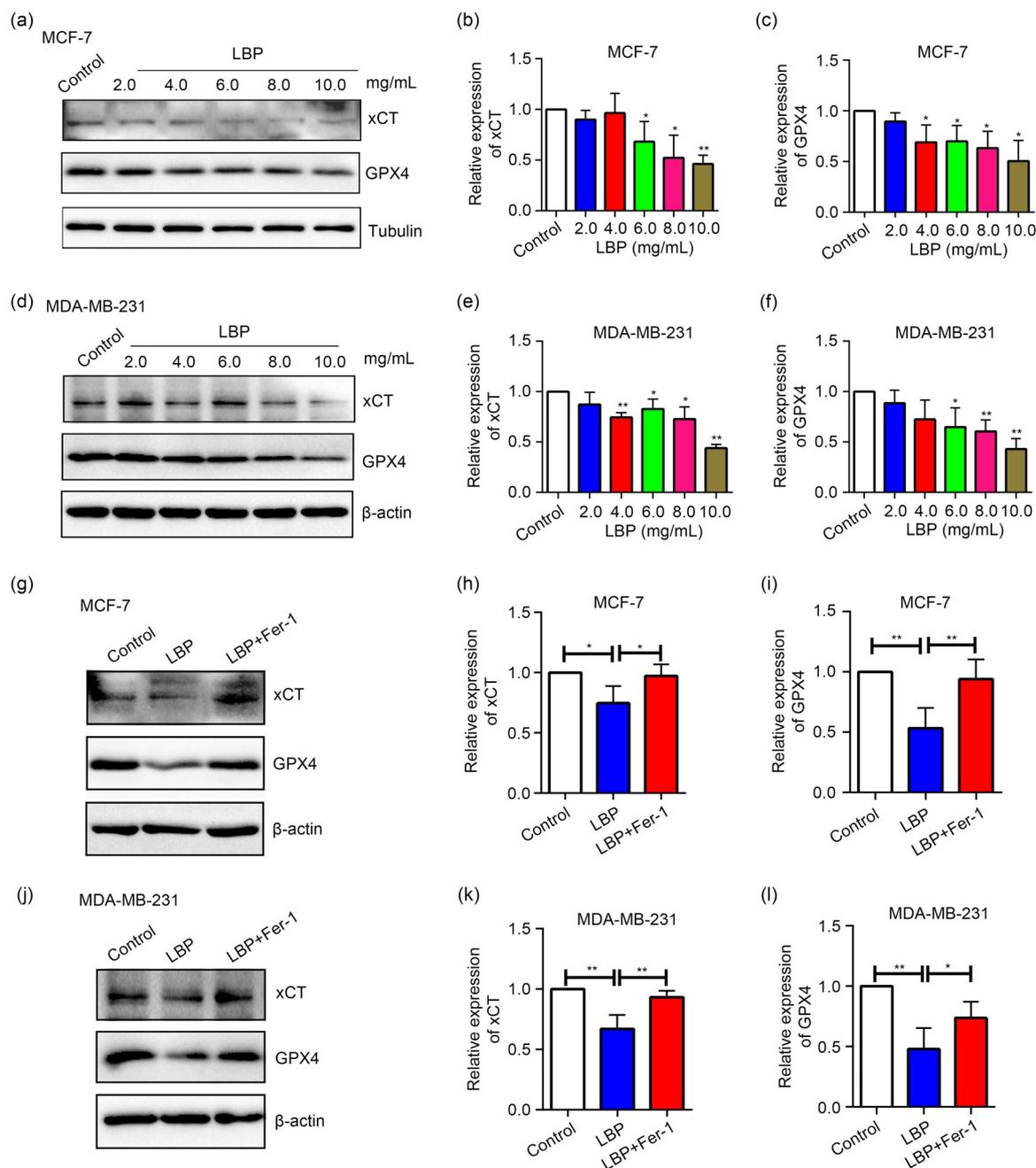
Fig. 6 Expression levels of light-chain subunit of cystine/glutamate antiporter system X$_c^-$ (xCT) and glutathione peroxidase 4 (GPX4) after treatment of breast cancer cells with *Lycium barbarum* polysaccharide (LBP). (a–c) Expression levels and quantification of xCT and GPX4 after treatment of MCF-7 cells with LBP; (d–f) Expression levels and quantification of xCT and GPX4 after treatment of MDA-MB-231 cells with LBP; (g–l) Expression levels and quantification of xCT and GPX4 were decreased by LBP treatment and rescued by Ferrostatin-1 (Fer-1) in MCF-7 (4.0 mg/mL LBP) and MDA-MB-231 (6.0 mg/mL LBP) cells. Data are expressed as mean±standard deviation (SD), *n*=3. (b, c, e, f) * *P*<0.05, ** *P*<0.01, compared with control; (h, i, k, l) * *P*<0.05, ** *P*<0.01.

To explore the relationship between ferroptosis occurrence and GPX4 and xCT expression under 4.0 mg/mL LBP treatment in MCF-7 cells and 6.0 mg/mL LBP in MDA-MB-231 cells, the cells were co-cultured with the specific ferroptosis inhibitor Fer-1 and LBP. The findings showed that xCT and GPX4 expression levels increased after suppression of ferroptosis in MCF-7 and MDA-MB-231 cells (Figs. 6g–6l). These results

indicated that LBP induces ferroptosis by modulating xCT and GPX4 expression.

3.6 LBP-induced ferroptosis through the xCT/GPX4 pathway in breast cancer cells

Inhibitors of xCT (Erastin) and GPX4 (RSL3) were added to MCF-7 cells and co-cultured with LBP to further verify whether LBP mediates xCT and GPX4 expression levels to induce ferroptosis in breast cancer cells. The findings showed that xCT and GPX4 inhibitors decreased expression levels of xCT and GPX4, respectively, and the expression levels were lower after LBP co-treatment with both inhibitors (Fig. 7). In summary, these findings implied that LBP induces ferroptosis in breast cancer cells through modulation of the xCT/GPX4 pathway.

4 Discussion

Traditional medicine has been used for the prevention and treatment of several human diseases, mainly in the form of anticancer therapies. Several anticancer drugs discovered in recent years are from natural or natural-based compounds (Dias et al., 2012; Newman and Cragg, 2020). A variety of natural anticancer drugs such as paclitaxel, lentinan, and camptothecin are extracted from plants, and the World Health Organization (WHO) reports that 250 000 species of medicinal plants are used for the treatment of different human diseases (WHO, 1999; Ijaz et al., 2018). Medicinal plants contain several compounds. Isolated bioactive compounds and semi-synthetic lead compounds are used as therapeutic anticancer drugs (Gezici and Şekeroğlu, 2019). Several effective antitumor drugs in clinical use, such as etoposide, paclitaxel, topotecan, and irinotecan, are derived from natural products. Their specific three-dimensional structures can bind to pathogenic proteins and inhibit their activity (Paterson and Anderson, 2005; Cragg and Pezzuto, 2015). In addition, natural products have higher specificity and efficacy compared with artificially designed and synthesized molecules (Paterson and Anderson, 2005). Therefore, natural bioactive compounds extracted from traditional Chinese herbal medicines are good candidates as anticancer drugs. LBP is the main effective ingredient extracted from *L. barbarum*, which is a traditional Chinese medicinal herb produced mostly in Ningxia, China. The *Compendium of Materia Medica* reported
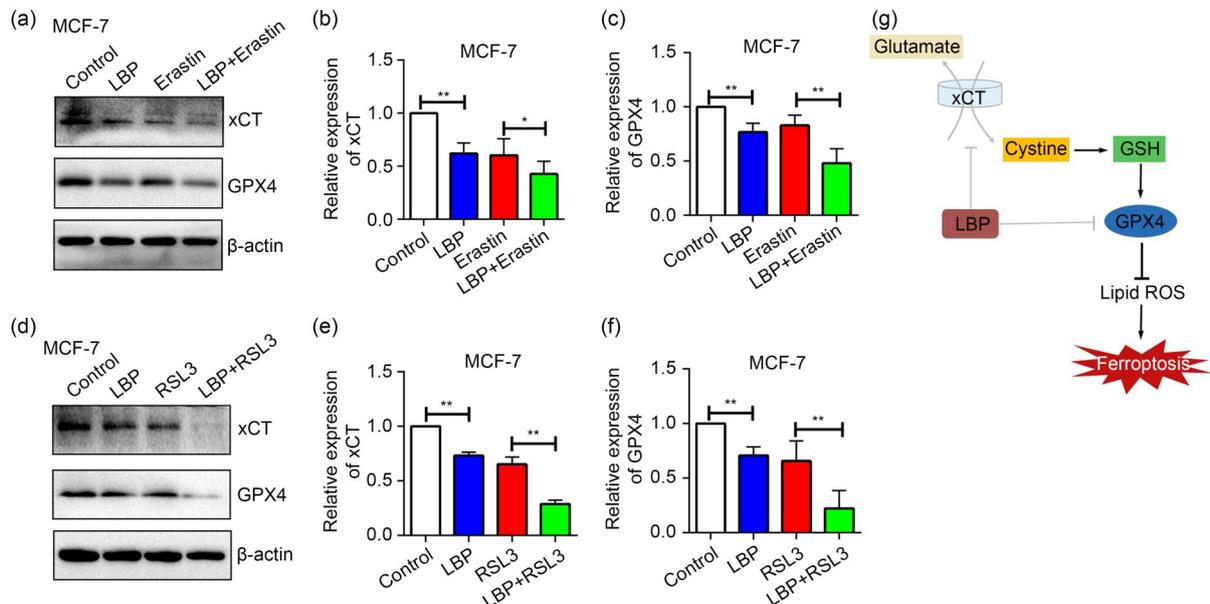

Fig. 7 *Lycium barbarum* polysaccharide (LBP) (4.0 mg/mL)-induced ferroptosis through the light-chain subunit of cystine/glutamate antiporter system X_c^- (xCT)/glutathione peroxidase 4 (GPX4) pathway in MCF-7 cells. (a–c) Expression levels and quantification of xCT and GPX4 after co-treatment of cells with LBP and Erastin (xCT inhibitor); (d–f) Expression levels and quantification of xCT and GPX4 after co-treatment of cells with LBP and RSL3 (GPX4 inhibitor); (g) Schematic representation of LBP-induced ferroptosis and related mechanisms in breast cancer cells. Data are expressed as mean± standard deviation (SD), *n*=3. * *P*<0.05, ** *P*<0.01. GSH: glutathione; ROS: reactive oxygen species.

that *L. barbarum* has important medicinal value in traditional Chinese medicine, and it is listed in the *Chinese Pharmacopoeia* in 2020 (Zhao et al., 2020; Ai et al., 2021). Although induction of apoptosis by LBP is the initial anticancer mechanism, induction of non-canonical cell death by several natural compounds has been explored in new anti-cancer strategies (Greco et al., 2021). In addition, LBP shows activity in inhibiting the growth of various tumor cells, and has several advantages such as low toxicity, fewer side effects, and high efficacy (Zhang et al., 2015; Wang et al., 2018). Therefore, LBP is a promising natural anticancer drug that exerts its activity by inducing atypical cell death. Ferroptosis is a novel type of non-canonical cell death that differs from apoptosis and autophagy. Various natural compounds induce ferroptosis in different in vitro and in vivo cancer models (Chen et al., 2020; Jin et al., 2020; Mbaveng et al., 2020). However, studies have not explored whether LBP causes ferroptosis in cancer cells. The findings of the current study showed that LBP induces ferroptosis in two types of breast cancer cells (MCF-7 and MDA-MB-231). To the best of our knowledge, this is the first study to explore the effects of LBP on ferroptosis of breast cancer cells.

The findings of this study showed that the lowest inhibiting concentration of LBP was 4.0 mg/mL for 48 h for MCF-7 and 6.0 mg/mL for 48 h for MDA-MB-231. A previous study reported that the lowest concentrations of LBP that significantly inhibited the growth of human gastric cancer cell lines MGC-803 and SGC-7901 were 100 and 200 mg/L, respectively (Miao et al., 2010). These findings were consistent with those from the current study showing differences in the sensitivity of the two types of cancer cells to LBP. In addition, LBP is significantly cytotoxic to human skin squamous carcinoma cells at concentrations of 400 μg/mL and above, whereas it significantly inhibits expression of proteins associated with proliferation within a dose range of 50 to 200 μg/mL (Zeng et al., 2019). Moreover, 300 μg/mL LBP significantly inhibits proliferation and the cell cycle of MCF-7 cells (Shen and Du, 2012). Analysis of LBP-treated murine colon cancer cell line CT26-WT showed that 100 μg/mL LBP significantly inhibited cell proliferation (Wang et al., 2018). Notably, a previous study reported that 6.25 mg/L LBP solution exerted the highest cell inhibition effect on human cervical cancer HeLa cells after 4 d of treatment

(Zhu and Zhang, 2013). In a study of LBP-treated human prostate cancer cell lines, concentrations from 100 to 1000 μg/mL LBP were applied and the findings showed that 200 μg/mL LBP significantly inhibited cell growth (Luo et al., 2009). Moreover, Zhang et al. (2017) reported that 200 μg/mL LBP inhibited proliferation and migration of bladder cancer cell line BIU87. Although the concentration of LBP was higher in the current study, the treatment time was shorter than 4 d as reported previously (Zhang et al., 2005). Variation in results among studies can be attributed to differences in the manufacture and purity of LBP in different studies. A review by Kwok et al. (2019) explored the use of LBP in previous studies and reported that differences in efficacy were attributed to the various sources of LBP, and that there was no research-grade LBP currently available in the market. The LBP used in most experiments was edible LBP powder purchased from various manufacturers. The purity of LBP varies significantly due to a lack of standard extraction and purification methods. The lack of standardized LBP sources and quality control implies that the experimental results will vary significantly based on the source.

Levels of Cyclin E and p21 of breast cancer cells were significantly affected by LBP treatment in the current study, indicating that LBP inhibited the proliferation of breast cancer cells by modulating the cell cycle, and arrested the cell cycle at the G1/S phase transition. Cyclin E binds cyclin-dependent-kinase 2 (CDK2) to promote cell transition from G1 phase to the S checkpoint (McDonald and El-Deiry, 2001). p21 is an inhibitor of CDK that suppresses activity of CDK and arrests cell cycle progression at G1/S phase (Lee et al., 2008). This finding is consistent with previous findings that LBP caused S phase arrest in human hepatoma cells (Deng et al., 2017), gastric cancer cells (Miao et al., 2010), and cervical cancer cells (Hu et al., 1994). However, another study reported that LBP promoted G0/G1 phase arrest in colon cancer cells (Mao et al., 2011). A previous study by Miao et al. (2010) reported that LBP caused changes in expression levels of Cyclin E and CDK2 proteins in human gastric cancer cells, which is consistent with the findings of the current study. Moreover, the p21 protein expression level was up-regulated in LBP-treated MCF-7 cells (Shen and Du, 2012). These findings indicate that LBP modulates the G1/S transition of the cell cycle and blocks the G1 phase.

Although several studies have explored the anti-cancer effects of LBP, the mechanisms of cancer cell death by LBP have not been fully elucidated. Ferroptosis is an important anti-cancer strategy, applied mainly by using natural products such as LBP that have no tolerance to cancer cells and have low toxicity. The findings of this study showed that LBP inhibited cell proliferation and blocked the cell cycle of two kinds of breast cancer cells, MCF-7 and MDA-MB-231. In addition, LBP induced lipid peroxidation and release of excessive free iron, which are markers of ferroptosis. A high level of free iron in cells is called a labile iron pool (LIP). A LIP can promote formation of lipid ROS through the Fenton reaction, thereby resulting in ferroptosis (Liu et al., 2021). In addition, the findings showed that LBP-induced ferroptosis in breast cancer cells was brought about by down-regulation of the expression of xCT and GPX4. Notably, these changes were rescued by the ferroptosis inhibitor Fer-1, and xCT and GPX4 inhibitors inhibited the expression of xCT and GPX4, respectively. This indicated that LBP induced ferroptosis in breast cancer cells by modulating the xCT/GPX4 pathway. GPX4 and xCT play a vital role in antagonizing ferroptosis by regulating the synthesis and antioxidation of GSH (Bridges et al., 2012; Yu and Long, 2016). GPX4 inactivity and repression of SLC7A11 (the gene for xCT) result in ROS accumulation, thereby modulating ferroptosis (Yang et al., 2014). A previous study reported that the natural product *Actinidia chinensis* Planch. (kiwifruit) induced ferroptosis in gastric cancer by inhibiting expression of GPX4 and xCT (Gao et al., 2020). However, more cellular and in vivo studies should be conducted to explore the complex pharmacological and toxicological characteristics of LBP.

5 Conclusions

The current study showed that LBP effectively inhibited proliferation of breast cancer cells and promoted ferroptosis by modulation of the xCT/GPX4 pathway. These indicate that LBP is a novel ferroptosis inducer, induces cell death, and inhibits proliferation of breast cancer cells. These findings provide a reference for the use of LBP in potential compound therapies for breast cancer treatment. In addition, the current study provides a basis for subsequent studies to explore the pharmacological mechanisms of action of LBP in other aspects of ferroptosis.

Author contributions

Xing DU, Jingjing ZHANG, Ling LIU, Bo XU, Hang HAN, Wenjie DAI, and Xiuying PEI performed the experimental research and data analysis. Xing DU, Shaozhang HOU, and Xufeng FU contributed to the study design, data analysis, and writing and editing of the manuscript. All authors have read and approved the final manuscript, and therefore, have full access to all the data in the study and take responsibility for the integrity and security of the data.

Compliance with ethics guidelines

Xing DU, Jingjing ZHANG, Ling LIU, Bo XU, Hang HAN, Wenjie DAI, Xiuying PEI, Xufeng FU, and Shaozhang HOU declare that they have no conflict of interest.

This article does not contain any studies with human or animal subjects performed by any of the authors.

References

Abotaleb M, Kubatka P, Caprnda M, et al., 2018. Chemotherapeutic agents for the treatment of metastatic breast cancer: an update. *Biomed Pharmacother*, 101:458-477. https://doi.org/10.1016/j.biopha.2018.02.108

Ai Y, Sun YN, Liu L, et al., 2021. Determination of biogenic amines in different parts of *Lycium barbarum* L. by HPLC with precolumn dansylation. *Molecules*, 26(4):1046. https://doi.org/10.3390/molecules26041046

Amagase H, Farnsworth NR, 2011. A review of botanical characteristics, phytochemistry, clinical relevance in efficacy and safety of *Lycium barbarum* fruit (Goji). *Food Res Int*, 44(7):1702-1717. https://doi.org/10.1016/j.foodres.2011.03.027

Arzi L, Hoshyar R, Jafarzadeh N, et al., 2020. Anti-metastatic properties of a potent herbal combination in cell and mice models of triple negative breast cancer. *Life Sci*, 243: 117245. https://doi.org/10.1016/j.lfs.2019.117245

Bai Z, Peng Y, Ye X, et al., 2022. Autophagy and cancer treatment: four functional forms of autophagy and their therapeutic applications. *J Zhejiang Univ-Sci B (Biomed & Biotechnol)*, 23(2):89-101. https://doi.org/10.1631/jzus.B2100804

Bridges RJ, Natale NR, Patel SA, 2012. System X_c^- cystine/glutamate antiporter: an update on molecular pharmacology and roles within the CNS. *Br J Pharmacol*, 165(1): 20-34. https://doi.org/10.1111/j.1476-5381.2011.01480.x

Chen P, Wu QB, Feng J, et al., 2020. Erianin, a novel dibenzyl compound in Dendrobium extract, inhibits lung cancer cell growth and migration via calcium/calmodulin-dependent ferroptosis. *Signal Transduct Target Ther*, 5:51. https://doi.org/10.1038/s41392-020-0149-3

Chen Q, Shi RL, Jiang DW, et al., 2017. *Lycium barbarum* polysaccharide inhibits gastric cancer cell proliferation, migration and invasion by down-regulation of MMPs and suppressing epithelial-mesenchymal transition. *Int J Clin Exp Pathol*, 10(7):7369-7374.

Corso CR, Mulinari Turin de Oliveira N, Moura Cordeiro L, et al., 2021. Polysaccharides with antitumor effect in breast cancer: a systematic review of non-clinical studies. *Nutrients*, 13(6):2008. https://doi.org/10.3390/nu13062008

Cragg GM, Pezzuto JM, 2015. Natural products as a vital source for the discovery of cancer chemotherapeutic and chemopreventive agents. *Med Princ Pract*, 25(Suppl 2): 41-59. https://doi.org/10.1159/000443404

Cumaoglu A, Bekci H, Ozturk E, et al., 2018. Goji berry fruit extracts suppress proliferation of triple-negative breast cancer cells by inhibiting EGFR-mediated ERK/MAPK and PI3K/Akt signaling pathways. *Nat Prod Commun*, 13(6):701-706. https://doi.org/10.1177/1934578X1801300613

Deng XL, Li XL, Luo S, et al., 2017. Antitumor activity of *Lycium barbarum* polysaccharides with different molecular weights: an in vitro and in vivo study. *Food Nutr Res*, 61:1399770. https://doi.org/10.1080/16546628.2017.1399770

Deng XL, Luo S, Luo X, et al., 2018. Polysaccharides from Chinese herbal *Lycium barbarum* induced systemic and local immune responses in H22 tumor-bearing mice. *J Immunol Res*, 2018:3431782. https://doi.org/10.1155/2018/3431782

Dias DA, Urban S, Roessner U, 2012. A historical overview of natural products in drug discovery. *Metabolites*, 2(2): 303-336. https://doi.org/10.3390/metabo2020303

Dixon SJ, Lemberg KM, Lamprecht MR, et al., 2012. Ferroptosis: an iron-dependent form of nonapoptotic cell death. *Cell*, 149(5):1060-1072. https://doi.org/10.1016/j.cell.2012.03.042

Du X, Xiao JJ, Fu XF, et al., 2021. A proteomic analysis of Bcl-2 regulation of cell cycle arrest: insight into the mechanisms. *J Zhejiang Univ-Sci B (Biomed & Biotechnol)*, 22(10):839-855. https://doi.org/10.1631/jzus.B2000802

Feng L, Xiao X, Liu J, et al., 2020. Immunomodulatory effects of *Lycium barbarum* polysaccharide extract and its uptake behaviors at the cellular level. *Molecules*, 25(6): 1351. https://doi.org/10.3390/molecules25061351

Gan L, Zhang SH, Yang XL, et al., 2004. Immunomodulation and antitumor activity by a polysaccharide–protein complex from *Lycium barbarum*. *Int Immunopharmacol*, 4(4): 563-569.

https://doi.org/10.1016/j.intimp.2004.01.023

Gao ZW, Deng GH, Li YJ, et al., 2020. *Actinidia chinensis* Planch prevents proliferation and migration of gastric cancer associated with apoptosis, ferroptosis activation and mesenchymal phenotype suppression. *Biomed Pharmacother*, 126:110092. https://doi.org/10.1016/j.biopha.2020.110092

García-Aranda M, Redondo M, 2019. Immunotherapy: a challenge of breast cancer treatment. *Cancers (Basel)*, 11(12): 1822. https://doi.org/10.3390/cancers11121822

Gezici S, Şekeroğlu N, 2019. Current perspectives in the application of medicinal plants against cancer: novel therapeutic agents. *Anti-Cancer Agents Med Chem*, 19(1):101-111. https://doi.org/10.2174/1871520619666181224121004

Greco G, Catanzaro E, Fimognari C, 2021. Natural products as inducers of non-canonical cell death: a weapon against cancer. *Cancers (Basel)*, 13(2):304. https://doi.org/10.3390/cancers13020304

Hu QH, Gao TS, Zhao CJ, et al., 1994. The effect of active components of *Lycium barbarum* and garlic (LB-GO) on the synthesis of DNA and ultrastructure of U_{14} cervix cancer cells in mice. *Chin J Cancer Res*, 6:266-273. https://doi.org/10.1007/BF03025580

Ijaz S, Akhtar N, Khan MS, et al., 2018. Plant derived anticancer agents: a green approach towards skin cancers. *Biomed Pharmacother*, 103:1643-1651. https://doi.org/10.1016/j.biopha.2018.04.113

Jin MM, Shi CZ, Li T, et al., 2020. Solasonine promotes ferroptosis of hepatoma carcinoma cells via glutathione peroxidase 4-induced destruction of the glutathione redox system. *Biomed Pharmacother*, 129:110282. https://doi.org/10.1016/j.biopha.2020.110282

Kumar P, Aggarwal R, 2016. An overview of triple-negative breast cancer. *Arch Gynecol Obstet*, 293(2):247-269. https://doi.org/10.1007/s00404-015-3859-y

Kwok SS, Bu YS, Lo ACY, et al., 2019. A systematic review of potential therapeutic use of *Lycium barbarum* polysaccharides in disease. *Biomed Res Int*, 2019:4615745. https://doi.org/10.1155/2019/4615745

Lee EJ, Moon GS, Choi WS, et al., 2008. Naringin-induced p21WAF1-mediated G_1-phase cell cycle arrest via activation of the Ras/Raf/ERK signaling pathway in vascular smooth muscle cells. *Food Chem Toxicol*, 46(12):3800-3807. https://doi.org/10.1016/j.fct.2008.10.002

Li J, Cao F, Yin HL, Huang ZJ, et al., 2020. Ferroptosis: past, present and future. *Cell Death Discov*, 11(2):88. https://doi.org/10.1038/s41419-020-2298-2

Liu ZX, Lv XY, Yang BW, et al., 2021. Tetrachlorobenzoquinone exposure triggers ferroptosis contributing to its neurotoxicity. *Chemosphere*, 264:128413. https://doi.org/10.1016/j.chemosphere.2020.128413

Lou L, Chen G, Zhong B, et al., 2019. *Lycium barbarum* polysaccharide induced apoptosis and inhibited proliferation in infantile hemangioma endothelial cells via down-regulation of PI3K/AKT signaling pathway. *Biosci Rep*,

39(8):BSR20191182.
https://doi.org/10.1042/BSR20191182

Luo Q, Li ZN, Yan J, et al., 2009. *Lycium barbarum* polysaccharides induce apoptosis in human prostate cancer cells and inhibits prostate cancer growth in a xenograft mouse model of human prostate cancer. *J Med Food*, 12(4):695-703.
https://doi.org/10.1089/jmf.2008.1232

Mao F, Xiao BX, Jiang Z, et al., 2011. Anticancer effect of *Lycium barbarum* polysaccharides on colon cancer cells involves G0/G1 phase arrest. *Med Oncol*, 28(1):121-126.
https://doi.org/10.1007/s12032-009-9415-5

Mbaveng AT, Chi GF, Bonsou IN, et al., 2020. *N*-Acetylglycoside of oleanolic acid (aridanin) displays promising cytotoxicity towards human and animal cancer cells, inducing apoptotic, ferroptotic and necroptotic cell death. *Phytomedicine*, 76:153261.
https://doi.org/10.1016/j.phymed.2020.153261

McDonald ER, El-Deiry WS, 2001. Checkpoint genes in cancer. *Ann Med*, 33(2):113-122.
https://doi.org/10.3109/07853890109002066

Miao Y, Xiao BX, Jiang Z, et al., 2010. Growth inhibition and cell-cycle arrest of human gastric cancer cells by *Lycium barbarum* polysaccharide. *Med Oncol*, 27(3):785-790.
https://doi.org/10.1007/s12032-009-9286-9

Newman DJ, Cragg GM, 2020. Natural products as sources of new drugs over the nearly four decades from 01/1981 to 09/2019. *J Nat Prod*, 83(3):770-803.
https://doi.org/10.1021/acs.jnatprod.9b01285

Paterson I, Anderson EA, 2005. The renaissance of natural products as drug candidates. *Science*, 310(5747):451-453.
https://doi.org/10.1126/science.1116364

Shen LL, Du G, 2012. *Lycium barbarum* polysaccharide stimulates proliferation of MCF-7 cells by the ERK pathway. *Life Sci*, 91(9-10):353-357.
https://doi.org/10.1016/j.lfs.2012.08.012

Shin SS, Hwang B, Muhammad K, et al., 2019. Nimbolide represses the proliferation, migration, and invasion of bladder carcinoma cells via Chk2-mediated G2/M phase cell cycle arrest, altered signaling pathways, and reduced transcription factors-associated MMP-9 expression. *Evid-Based Complement Alternat Med*, 2019:3753587.
https://doi.org/10.1155/2019/3753587

Tabor S, Szostakowska-Rodzos M, Fabisiewicz A, et al., 2020. How to predict metastasis in luminal breast cancer? Current solutions and future prospects. *Int J Mol Sci*, 21(21):8415.
https://doi.org/10.3390/ijms21218415

Tavsan Z, Kayali HA, 2019. Flavonoids showed anticancer effects on the ovarian cancer cells: involvement of reactive oxygen species, apoptosis, cell cycle and invasion. *Biomed Pharmacother*, 116:109004.
https://doi.org/10.1016/j.biopha.2019.109004

Wang W, Liu MX, Wang Y, et al., 2018. *Lycium barbarum* polysaccharide promotes maturation of dendritic cell via Notch signaling and strengthens dendritic cell mediated

T lymphocyte cytotoxicity on colon cancer cell CT26-WT. *Evid Based Complement Alternat Med*, 2018:2305683.
https://doi.org/10.1155/2018/2305683

WHO, 1999. WHO Monographs on Selected Medicinal Plants. World Health Organization, Geneva.

Xu J, Wu KJ, Jia QJ, et al., 2020. Roles of miRNA and lncRNA in triple-negative breast cancer. *J Zhejiang Univ-Sci B (Biomed & Biotechnol)*, 21(9):673-689.
https://doi.org/10.1631/jzus.B1900709

Yang WS, SriRamaratnam R, Welsch ME, et al., 2014. Regulation of ferroptotic cancer cell death by GPX4. *Cell*, 156(1-2):317-331.
https://doi.org/10.1016/j.cell.2013.12.010

Yang WS, Kim KJ, Gaschler MM, et al., 2016. Peroxidation of polyunsaturated fatty acids by lipoxygenases drives ferroptosis. *Proc Natl Acad Sci USA*, 113(34):E4966-E4975.
https://doi.org/10.1073/pnas.1603244113

Yu XL, Long YC, 2016. Crosstalk between cystine and glutathione is critical for the regulation of amino acid signaling pathways and ferroptosis. *Sci Rep*, 6:30033.
https://doi.org/10.1038/srep30033

Zeng MH, Kong QT, Liu F, et al., 2019. The anticancer activity of *Lycium barbarum* polysaccharide by inhibiting autophagy in human skin squamous cell carcinoma cells *in vitro* and *in vivo*. *Int J Polym Sci*, 2019:5065920.
https://doi.org/10.1155/2019/5065920

Zhang M, Chen HX, Huang J, et al., 2005. Effect of *Lycium barbarum* polysaccharide on human hepatoma QGY7703 cells: inhibition of proliferation and induction of apoptosis. *Life Sci*, 76(18):2115-2124.
https://doi.org/10.1016/j.lfs.2004.11.009

Zhang Q, Lv XL, Wu T, et al., 2015. Composition of *Lycium barbarum* polysaccharides and their apoptosis-inducing effect on human hepatoma SMMC-7721 cells. *Food Nutr Res*, 59:28696.
https://doi.org/10.3402/fnr.v59.28696

Zhang XJ, Yu HY, Cai YJ, et al., 2017. *Lycium barbarum* polysaccharides inhibit proliferation and migration of bladder cancer cell lines BIU87 by suppressing Pi3K/AKT pathway. *Oncotarget*, 8(4):5936-5942.
https://doi.org/10.18632/oncotarget.13963

Zhao JC, Jin Y, Yan YM, et al., 2020. Herbal textual research on "Lycii Fructus" and "Lycii Cortex" in Chinese classical prescriptions. *Mod Chin Med*, 22(8):1269-1286 (in Chinese).
https://doi.org/10.13313/j.issn.1673-4890.20200422005

Zhu CP, Zhang SH, 2006. The antitumor and immunoenhancement activity of *Lycium barbarum* polysaccharides in hepatoma H_{22}-bearing mice. *Acta Nutr Sin*, 28(2):182-183 (in Chinese).
https://doi.org/10.3321/j.issn:0512-7955.2006.02.033

Zhu CP, Zhang SH, 2013. *Lycium barbarum* polysaccharide inhibits the proliferation of HeLa cells by inducing apoptosis. *J Sci Food Agric*, 93(1):149-156.
https://doi.org/10.1002/jsfa.5743